

Supporting Information

3D printable magnetic hydrogels with adjustable stiffness and adhesion for magnetic actuation and magnetic hyperthermia applications

**Xueting Xuan ^a, Yi Li ^b, Xing Xu ^c, Zhouyi Pan ^b, Yu Li ^b, Yonghao Luo ^{d*}, and Li
Sun ^{e**}**

^a School of Health Science and Engineering, University of Shanghai for Science and Technology, Shanghai 200093, China

^b College of Materials and Textile Engineering & Nanotechnology Research Institute, Jiaxing University, Jiaxing 314001, China

^c School of Materials Science and Intelligent Engineering, Nanjing University, Suzhou 215163, China

^d School of Chemistry and Chemical Engineering, Key Laboratory for Green Processing of Chemical Engineering of Xinjiang Bingtuan, Shihezi University, Shihezi 832004, China

^e Department of Mechanical and Aerospace Engineering, University of Houston, Houston, Texas 77204, USA

*Corresponding author: Y. H. Luo and L. Sun

Address: University of Houston, Houston, Texas, USA

Telephone: 7137434509

Email: lsun4@uh.edu (L.Sun) and luoyonghao@dlut.edu.cn (Y. H. Luo)

Table S1. The composition of PAM-Fe₃O₄ magnetic hydrogels.

Hydrogels	AM (g)	Fe ₃ O ₄ + Water (g)	MBA (g)	APS (g)	TEMED (μ L)	Total (g)
23 wt% PAM		0 + 23				
23 wt% PAM-5 wt% Fe ₃ O ₄		6 + 17				
23 wt% PAM-10 wt% Fe ₃ O ₄	6.9	12 + 11	0.0153	0.0129	22.2	30
23 wt% PAM-15 wt% Fe ₃ O ₄		18 + 5				
18.4 wt% PAM		0 + 30.5				
18.4 wt% PAM-5 wt% Fe ₃ O ₄		7.5 + 23				
18.4 wt% PAM-10 wt% Fe ₃ O ₄	6.9	15 + 15.5	0.0153	0.0129	22.2	37.5
18.4 wt% PAM-15 wt% Fe ₃ O ₄		22.5 + 8				
13.8 wt% PAM		0 + 43				
13.8 wt% PAM-5 wt% Fe ₃ O ₄		10 + 33				
13.8 wt% PAM-10 wt% Fe ₃ O ₄	6.9	20 + 23	0.0153	0.0129	22.2	50
13.8 wt% PAM-15 wt% Fe ₃ O ₄		30 + 13				

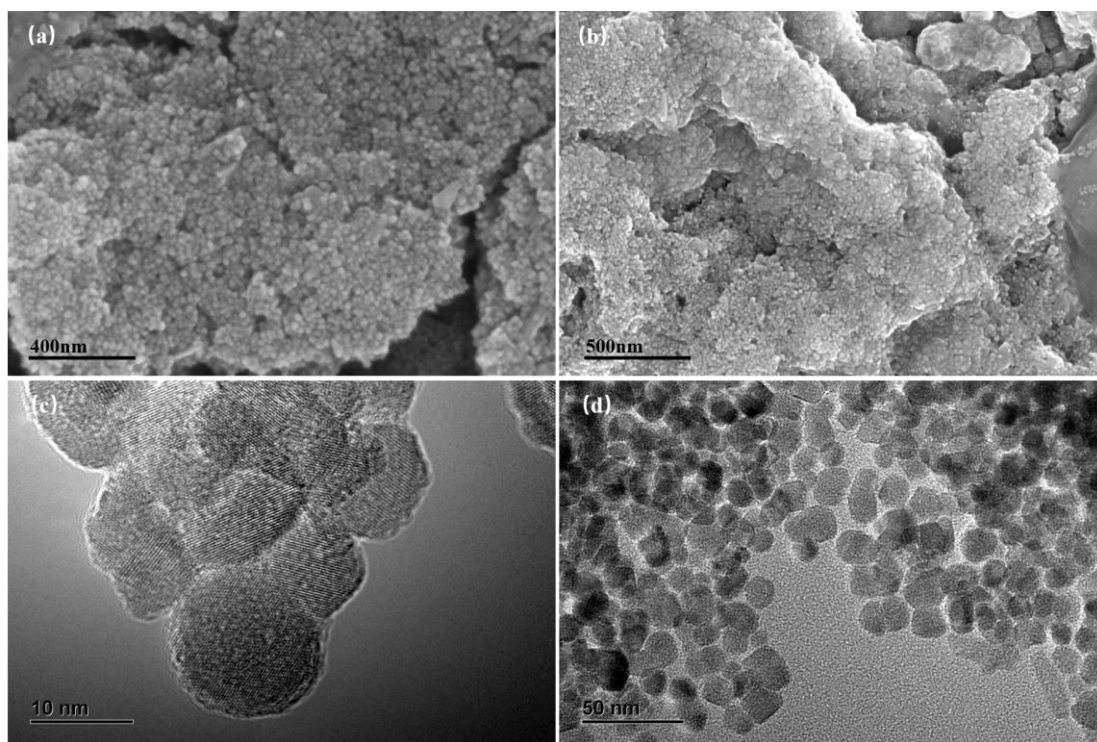


Figure S1. The SEM images of (a-b) SEM images of 25 wt% Fe₃O₄ dispersion, (c-d) TEM images of 25 wt% Fe₃O₄ dispersion.

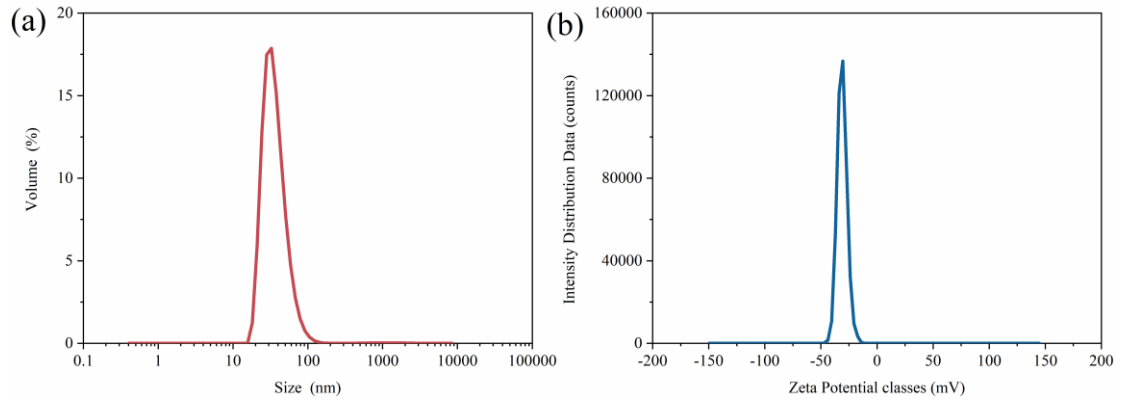


Figure S2. (a) Particle size distribution of Fe_3O_4 in 25 wt% Fe_3O_4 dispersion, (b) Zeta potential of 25 wt% Fe_3O_4 dispersion.

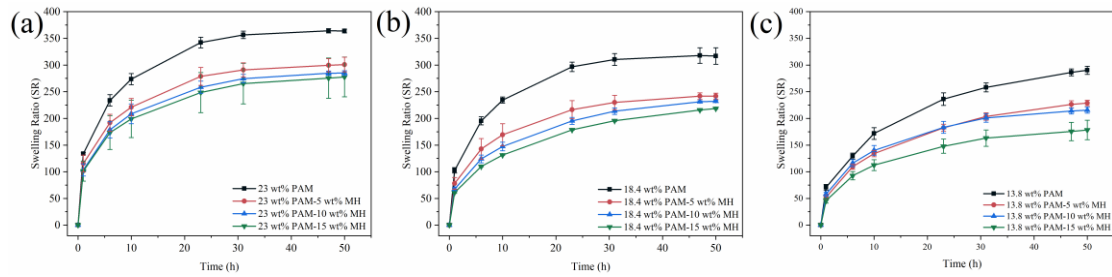


Figure S3. The swelling ratio versus time curves of PAM- Fe_3O_4 magnetic hydrogels with different concentrations at different times.

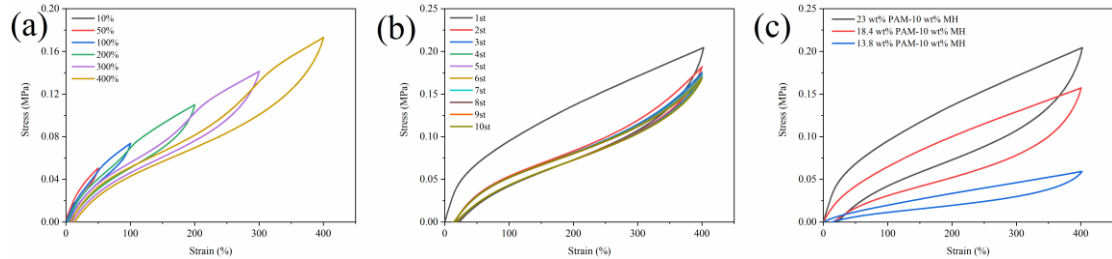


Figure S4. Tensile cycling experiment of PAM- Fe_3O_4 magnetic hydrogels. (a) Tensile cycling experiments of 23 wt% PAM-10 wt% MH under different strains, (b) tensile cycling experiment of 23 wt% PAM-10 wt% MH at 400% strain for 10 times, (c) 23 wt% PAM-10 wt% MH, 18.4 wt% PAM-10 wt% MH, 13.8 wt% PAM-10 wt% MH were cycled once at 400% tensile strain.

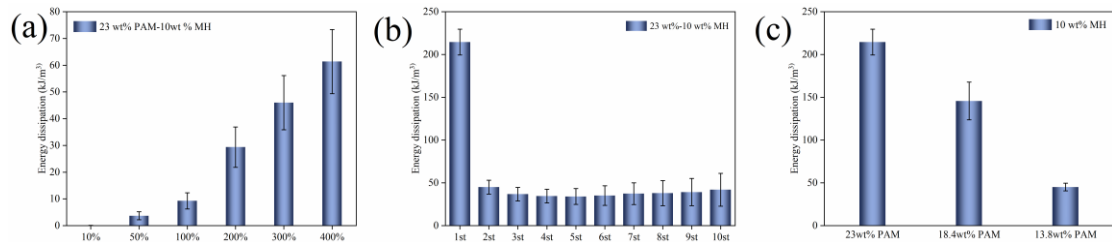


Figure S5. Energy dissipation of the stretching cycle of PAM- Fe_3O_4 magnetic hydrogels. (a) Energy dissipation of 23 wt% PAM-10 wt% MH during stretching

cycles under different strains, (b) energy dissipation test of 23 wt% PAM-10 wt% MH after 10 stretching cycles at 400% strain, (c) energy dissipation of 23 wt% PAM-10 wt% MH, 18.4 wt% PAM-10 wt% MH, 13.8 wt% PAM-10 wt% MH after one cycle at 400% tensile strain.

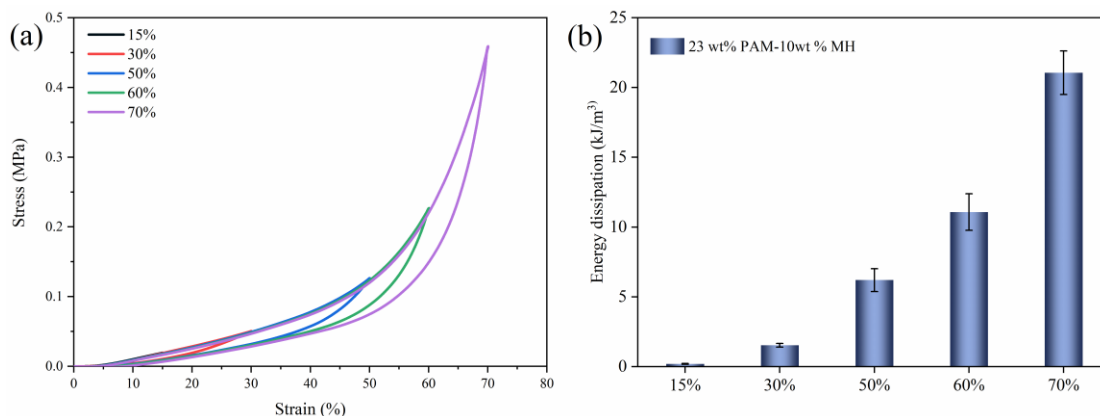


Figure S6. Compression cycle of PAM-Fe₃O₄ magnetic hydrogels. (a) Compression cycles of 23 wt% PAM-10 wt% MH under different strains, (b) energy dissipation of 23 wt% PAM-10 wt% MH during compression cycle under different strains.

Table S2. 3D printing parameters of PAM-Fe₃O₄ magnetic hydrogels.

Hydrogel structures	Printing needle	Printing pressure	Printing speed	Model size	Printing layers
Square frame				10 mm × 10 mm	20 layers
Triangular pyramid	inner diameter of 0.41 mm	0.1 MPa	15 mm/s	20 mm × 20 mm	20 layers
mesh structure				20 mm × 20 mm	15 layers
				25 mm × 25 mm	10 layers